

## Sintering and Grain Growth Behaviour of Ultra Fine Al<sub>2</sub>O<sub>3</sub> Powder

Mehdi Mazaheri<sup>1,2</sup>, Z. Razavi Hesabi<sup>1</sup>, M. Haghightzadeh<sup>1</sup>, S.K. Sadrnezhaad<sup>1</sup>

<sup>1</sup>Materials and Energy Research Center, Tehran, Iran

<sup>2</sup>Institute of Physics of Complex Matter, Swiss Federal Institute of Technology Lausanne (EPFL)  
1015 Lausanne, Switzerland

### Abstract

The sub micrometer alumina powder with an average particle size of 150 nm was sintered using two different methods, i.e. conventional sintering (CS) and two-step sintering (TSS). While the grain size of full-dense structures produced by conventional sintering ranges between 1-2  $\mu\text{m}$ , the application of an optimum TSS regime led to a remarkable decrease of grain size down to  $\sim 500$  nm. The results show that low temperature isothermal dwell at 1150°C after heating the green compacts up to 1300°C decreased the grain size from 1.2  $\mu\text{m}$  to 850 nm. A further decrease of the first step temperature to 1250°C led to the formation of a finer structure with an average grain size of 500 nm.

### Introduction

The outstanding attention that nanostructured materials have recently drawn stem from their useful mechanical, physical, optical, and magnetic properties [1-6]. These splendid characteristics stimulate several applications in different technological fields, such as in electronics, catalysis, magnetic data storage, energy storage, structural components and ceramics [7, 8]. The high surface area of nanoparticles additionally supplies a substantial sintering driving force by which the sintering temperature can be decently lowered [9-13]. From the mechanical point of view, contrary to the brittleness of micro-grained ceramics, nanometer-grained ones are typically capable of putting up with important elongation before breaking at moderate temperatures ( $\sim 0.5 T_m$ ) [7, 14].

From the thermodynamics concept, in the temperature range where the grain boundary diffusion is active while grain boundary migration is sufficiently sluggish, densification would continue without any significant grain growth. On the basis of this idea, Chen and Wang [15] developed a novel technique, called two-step sintering (TSS), to suppress the accelerated grain growth at the final stage of sintering by triple junctions. To take the advantage of boundary dragging by triple junctions, at first a critical density should be achieved where sufficient triple junctions exist throughout the body as pins. Then with decreasing the sintering temperature to a critical degree, the grain-growth would be stopped by triple junctions while densification may not be impaired. In doing so, samples have to be exposed to prolonged isothermal heating at the second, low temperature step. Referring to conducted successful TSS in open literature, different critical densities were reported for various systems. For instance, Chen and Wang [15] determined the density of 75% theoretical

density (TD) as the critical one for TSS of nano-yttria to succeed. Li and Ye [16] reported that below 82% TD, alumina nanopowder would not be densified even after prolonged soaking in the second step. As in a TSS regime, the triple junctions are going to prohibit grain growth while unstable pores can shrink with low temperature annealing; seemingly the source of different densities lies in the pore size and distribution which needs to be further investigated. Certainly, the formation of inhomogeneous porosity due to the increased tendency of nanopowder to form agglomerates complicates the situation. To solve this problem, one can use larger particles with a lower agglomeration degree and shape green bodies with advanced methods to obtain a more homogenous structure. Under this condition one can expect successful TSS at lower temperatures.

In the present study, two step sintering was applied on sub-micrometer Al<sub>2</sub>O<sub>3</sub> powder to achieve a dense ultrafine structure. The sintering behavior and structural evolution during densification were traced. The effect of temperature of both sintering steps on densification and grain growth at different TSS regimes were discussed. Hardness and fracture toughness of two-step sintered samples were reported.

### Experimental

Alumina powder (Taimicron TM-DAR; Taimei Chemicals Co., Ltd., Tokyo, Japan) with a mean particle size of 150 nm was used. The morphology of the powder was examined with a scanning electron microscopy (SEM, Philips XL30, the Netherlands). The powder was firstly shaped in a cylindrical die with 10 mm diameter under uniaxial pressure of 50 MPa. The preformed green samples were then cold isostatic pressed under 200 MPa. Sintering of the green bodies shaped through CIP was carried out by conventional sintering (CS) and two-step sintering (TSS) methods. CS specimens were non-isothermally sintered between 1050 and 1400°C in air with a heating ramp of 10°C·min<sup>-1</sup>. Different two-step sintering regimes were applied to minimize the final grain size. On the first step, pellets were heated up to  $T_1$  with a heating ramp of 10°C·min<sup>-1</sup>. They were then cooled down to the lower temperatures of  $T_2$  with a cooling rate of 50°C·min<sup>-1</sup> and soaked for a prolonged period of time. Table 1 lists the conditions under which TSS regimes were carried out. The density of the sintered samples was measured by Archimedes method in water. To prevent penetration of water to open pores, these were sealed by smearing the specimens' surface with wax. The sintered grain size was determined from SEM

micrographs (the mean diameter of grains was measured) of fracture surfaces, counting at least 150 grains for each specimen. At least three specimens were measured, and the average values are reported as the result.

Table 1 The conditions for TSS regimes.

TSS regime	$T_1$ , °C	$T_2$ , °C	Maximum holding time at $T_2$ , h
TSS1	1300	1200	15
TSS2	1300	1100	15
TSS3	1300	1150	50
TSS4	1200	1150	15
TSS5	1250	1150	64

## Results and Discussion

Fig. 1 shows the SEM micrograph of the as-received sub-micrometer (150 nm) alumina powder. As it can be seen, no tight agglomeration can be observed.

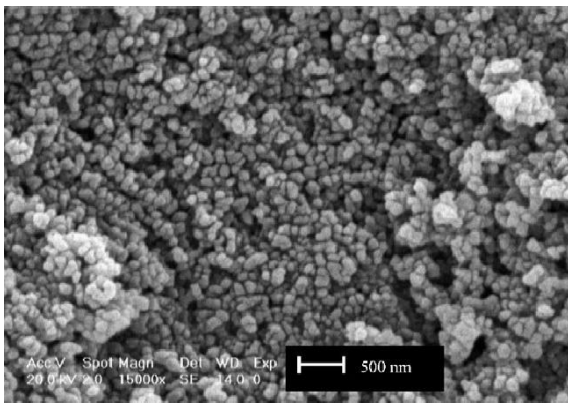


Fig. 1 SEM micrograph of ultra pure alumina powder.

Fig. 2 shows the structural evolution of green compacts shaped via CIP while firing through heating up to 1400°C with a heating rate of 10°C min<sup>-1</sup>. Up to 1250°C, no obvious change in grain size was observed while a significant increase in density occurred. A further increase of temperature (1300°C) yielded a density of ~ 87% TD and a grain size of ~ 350 nm. Densification was, however, nearly complete (~ 98% TD) at 1400 °C without isothermal dwelling. The final grain size of the nearly-fully dense structure was higher than 1.2 μm. In other words, 11% increase of relative fired density (from ~ 87% to ~ 98% TD) led to a remarkable grain growth of more than 240% (from ~ 350 nm to ~ 1.2 μm). To suppress the grain growth, different two-step sintering regimes were applied to densify green compacts without the accelerated grain growth at the final stage of sintering. In doing so, long time isothermal dwell at lower temperatures instead of continuous heating up/isothermal dwelling at a constant temperature was reported to be effective.

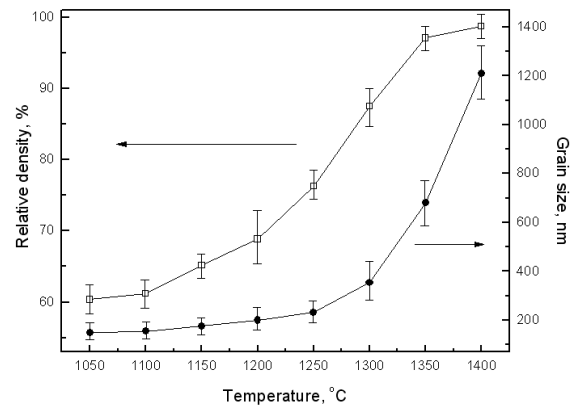


Fig. 2 Fractional density and grain size of sub-micron Al<sub>2</sub>O<sub>3</sub> green compacts through heating up with a constant heating ramp of 10°C/min.

Fig. 3 shows the variation of fractional fired density and grain size versus holding time at 1200°C for samples firstly heated up to 1300°C (TSS1). Although the temperature was decreased by 100°C in the second step, a significant grain growth was observed. In other words, the coarse structure with an average grain size of ~ 1.1 μm was obtained, comparable to that achieved via continuous heating up to 1400°C. The maximum relative density of both samples was ~ 98% TD. To succeed in inhibiting the grain growth, the second step temperature was decreased further to 1100°C (TSS2). As observed (Fig. 4), even after 16 h soaking at 1100°C only a slight increase in density was achieved. Most obviously, the second step temperature was not sufficient for elimination of the residual porosity. Figs. 3 and 4 illustrate how important the temperate of the second step might be. Not only did low temperature isothermal dwell in the second step fail to eliminate the residual porosity but also high temperature soaking led to an uncontrolled grain growth. Seemingly, there is a critical temperature between 1100°C and 1200°C which could be chosen as the second step temperature for elimination of the residual porosity without accelerated grain growth.

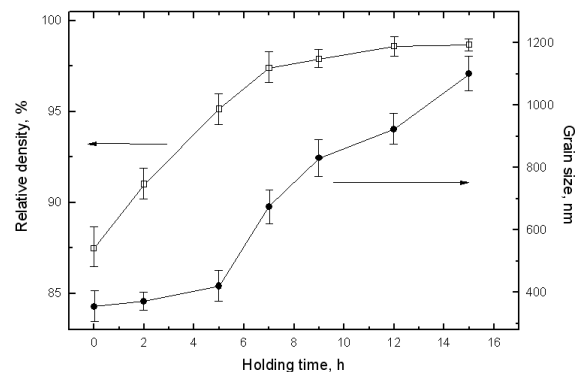


Fig. 3 Fractional fired density and grain size versus holding time at 1200°C for sub-micron Al<sub>2</sub>O<sub>3</sub> green compacts firstly heated up to 1300°C (TSS1).

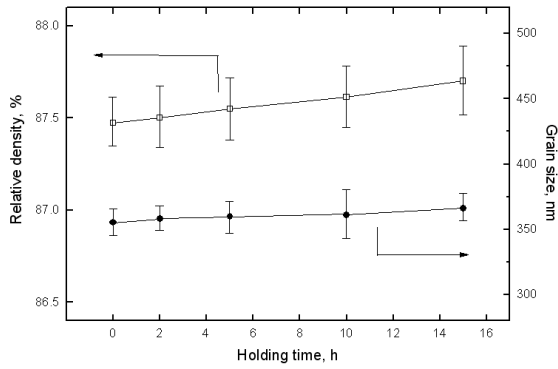


Fig. 4 Fractional fired density and grain size versus holding time at 1100°C for sub-micron Al<sub>2</sub>O<sub>3</sub> green compacts firstly heated up to 1300 °C (TSS2).

Fig. 5 shows the results of density and grain size measurement for TSS3 cycle conducted at  $T_1=1300^\circ\text{C}$  and  $T_2=1150^\circ\text{C}$  ( $1100^\circ\text{C} < T_2 < 1200^\circ\text{C}$ ). After 50 h dwell at 1150°C, green compacts were densified and relatively finer structures with an average grain size of ~ 0.85 μm were obtained. To find how effective the first step temperature might be,  $T_1$  was decreased from 1300°C down to 1200°C (TSS4).

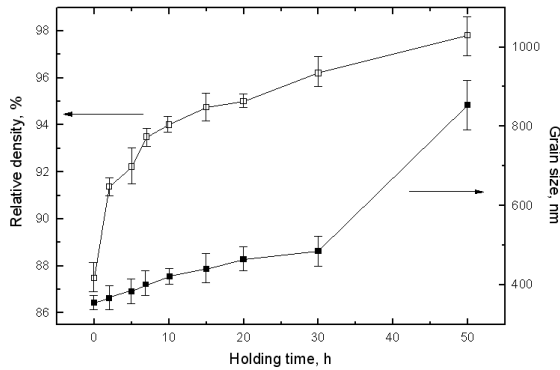


Fig. 5 Fractional fired density and grain size versus holding time at 1150°C for sub-micron Al<sub>2</sub>O<sub>3</sub> green compacts firstly heated up to 1300 °C (TSS3).

Fig. 6 shows the effect of decreasing the temperature of the first step on densification and grain growth versus holding time. With decreasing the temperature in the first step, the density (obtained at the end of the first step) was decreased from ~ 87.5% TD to ~ 69% TD. After 9 h soaking at 1150°C the density increased up to ~ 90% TD while further soaking did not affect densification any more. The grain size was increased from ~ 200 nm to ~ 310 nm. The results indicate that the initial density after the first step was lower than the critical one, which resulted in failure of the procedure. To increase the initial density, the samples were heated up to 1250°C. Fig. 7 shows structural evolution of green compacts firstly fired through heating up to 1250°C, followed by holding at 1150°C (TSS5). Successfully, 50°C increase of the first step temperature led to the formation of a nearly-full dense structure with an average grain size of ~ 500 nm. The final density of sintered bodies achieved 98% TD.

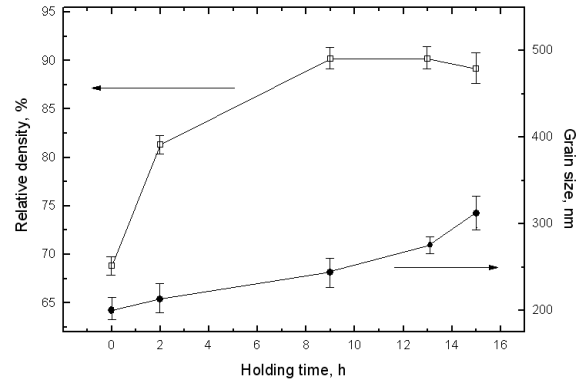


Fig. 6 Fractional fired density and grain size versus holding time at 1150°C for sub-micron Al<sub>2</sub>O<sub>3</sub> green compacts firstly heated up to 1200°C (TSS4).

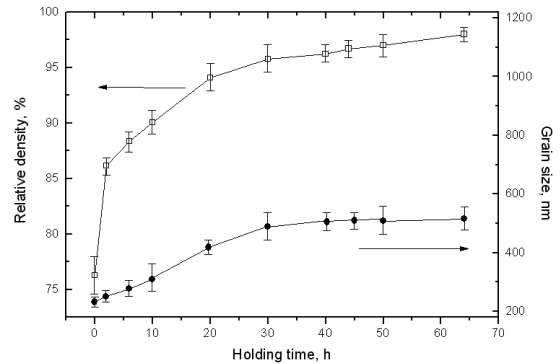


Fig. 7 Fractional fired density and grain size versus holding time at 1150°C for sub-micron Al<sub>2</sub>O<sub>3</sub> green compacts firstly heated up to 1250°C (TSS5).

Two-step sintering results show that there is a critical temperature for the second step as well as for the first one. For instance, low temperature isothermal dwelling at 1100°C in the second step failed to eliminate the residual porosity of samples which were firstly heated up to 1300°C (TSS2). High temperature soaking at 1200°C led to an accelerated grain growth (TSS1), while with further decrease of the second temperature ( $T_2$ ) the two-step sintering was successfully conducted (TSS3). Fig. 7 shows that initial density of 75% TD is sufficient for removal of pores in the second step (TSS3).

Fig. 8 summarizes the effect of different TSS regimes on sintering paths of sub-micron alumina compared with that obtained through continuous heating. It is shown how effectively the temperatures of the two sintering steps in TSS cycles affect the densification and grain growth. Fig. 9 shows the SEM micrograph of samples sintered under optimum TSS regime (TSS5).

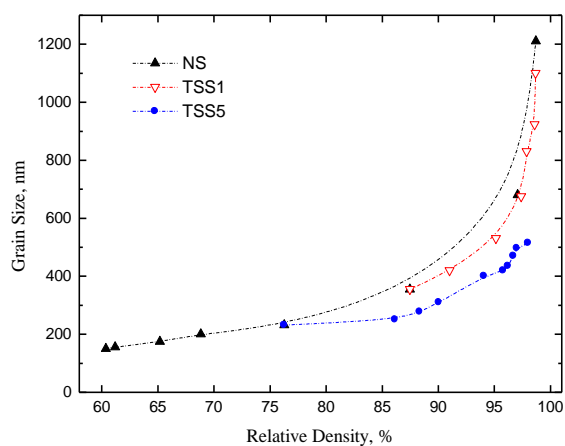


Fig. 8 Structural evolution of sub-micron  $\text{Al}_2\text{O}_3$  green compacts through heating up to  $1400^\circ\text{C}$  and different TSS heating regimes.

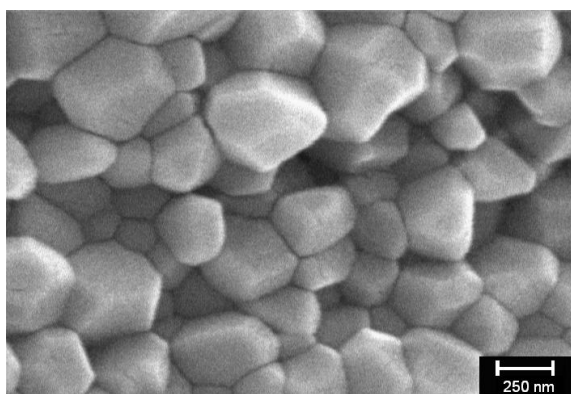


Fig. 9 SEM picture of sintered sub-micron  $\text{Al}_2\text{O}_3$  under TSS5 regime (The green sample firstly heated up to  $T_1=1250^\circ\text{C}$ , cooled down to  $T_2=1150^\circ\text{C}$  and held at  $T_2$  for 64 h).

## Conclusions

The sub-micrometer  $\text{Al}_2\text{O}_3$  powder with an average particle size of 150 nm was sintered via the two-step sintering method. To obtain the minimum grain size different TSS cycles were designed. The structural evolution during sintering was traced. The results show that low temperature isothermal dwell at  $1150^\circ\text{C}$ , after heating the green compacts up to  $1300^\circ\text{C}$ , decreased the grain size from  $1.2\ \mu\text{m}$  down to 850 nm. A further decrease of the first step temperature to  $1250^\circ\text{C}$  led to the formation of a finer structure with an average grain size of 500 nm.

## References

1. R. Vaben, D. Stover, Processing and properties of nanophase ceramics, *J. Mater. Process. Tech.* **92** (1999) 77-84.
2. M. Salavati-Niasari, F. Davar, M. Mazaheri, M. Shaterian, Preparation of cobalt nanoparticles from [bis(salicylidene)cobalt(II)]- oleylamine complex by thermal decomposition, *J. Mag. Mag. Mater.* **320** (2007) 575-578.
3. J. Karch, R. Bringer, H. Gleiter, ceramics ductile at low temperatures, *Nature* **330** (1987) 556-558.

4. M.J. Mayo, D.C. Hague, D.J. Chen, Processing Nanocrystalline Ceramics for Application in Superplasticity, *Mater. Sci. Eng.* **A166** (1993) 145-159.
5. M.J. Mayo, Synthesis and applications of nanocrystalline ceramics, *Mater. Design* **14** (1993) 323-329.
6. Y. Sakka, T.S. Suzuki, K. Morita, K. Nakano, K. Hiraga, Colloidal processing and superplastic properties of zirconia and alumina-based nanocomposites, *Scripta Mater.* **44** (2001) 2075-2078.
7. A. Weibel, R. Bouchet, P. Bouvier, P. Knauth, Hot compaction of nanocrystalline  $\text{TiO}_2$  (anatase) ceramics. Mechanisms of densification: Grain size and doping effects, *Acta Mater.* **54** (2006) 3575-3583.
8. S. Yang, L. Gao, Preparation of Titanium Dioxide Nanocrystallite with High Photocatalytic Activities, *J. Amer. Ceram. Soc.* **88** (2005) 968-970.
9. M. Mazaheri, A.M. Zahedi, S.K. Sadrnezhad, Two-Step Sintering of Nanocrystalline ZnO Compacts: Effect of Temperature on Densification and Grain Growth, *J. Am. Ceram. Soc.* **91** (2008) 56-63.
10. J.R. Groza, Nanosintering, *Nanostruc. Mater.* **12** (1999) 987-992.
11. K. Maca, M. Trunec, P. Dobask, Bulk Zirconia Nanoceramics Prepared by Cold Isostatic Pressing and Pressureless Sintering, *Rev. Adv. Mater. Sci.* **10** (2005) 84-88.
12. D. Jiang, M. J. Mayo, Rapid Rate Sintering of Nanocrystalline  $\text{ZrO}_2$ -3mol%  $\text{Y}_2\text{O}_3$ , *J. Amer. Ceram. Soc.* **79** (1996) 906-912.
13. M. Mazaheri, A. Simchi, M. Dourandish, F. G-Fard, Master Sintering Curve for Nanocrystalline 3Y-TZP Powder Compacts, *Ceram. Int.* (2008) *in press*.
14. M.J. Mayo, D.J. Chen, D.C. Hague., Edited by: A.S. Edelstein, R.C. Cammarata. *Nanomaterials: synthesis, properties and applications*. Bristol, UK: Institute of Physics Publishing; 1996. p. 191.
15. I.-W. Chen, X.-H. Wang, Sintering dense nanocrystalline ceramics without final-stage grain growth, *Nature* **404** (2000) 168-171.
16. J. Li, Y. Ye, Densification and grain growth of  $\text{Al}_2\text{O}_3$  nanoceramics during pressureless sintering, *J. Am. Ceram. Soc.* **89** (2006) 139-143.

\*Corresponding author:

Mehdi Mazaheri

Tel: +41 783 088880

[mehdi.mazaheri@epfl.ch](mailto:mehdi.mazaheri@epfl.ch)